Journal of Physics: Conference Series

PAPER • **OPEN ACCESS**

Impact of Mn-Pn intermixing on magnetic properties of an intrinsic magnetic topological insulator: the μSR perspective

To cite this article: M Sahoo *et al* 2023 *J. Phys.: Conf. Ser.* **2462** 012040

Impact of Mn-Pn intermixing on magnetic properties of an intrinsic magnetic topological insulator: the μSR perspective

M Sahoo[1,3],Z Salman[2], G Allodi[3], A Isaeva[1,4], L Folkers[4,5], AUB Wolter[1], B Büchner[1], R De Renzi[3]

[1] Leibniz IFW Dresden, 01069 Dresden, Germany.
[2] Laboratory for Muon Spin Spectroscopy, Paul-Scherrer-Institute, CH-5232 Villigen PSI, Switzerland.
[3] Dipartimento di Scienze Matematiche, Fisiche ed Informatiche, Universit'a di Parma, Parco Area delle Scienze 7A, I-43100 Parma, Italy.
[4] Van der Waals-Zeeman Institute, University of Amsterdam,The Netherlands
[5] Institut für Festkörper und Materialphysik, Technische Universität Dresden,Germany

E-mail: `manaswini.sahoo@unipr.it`

Abstract. We investigated the magnetic properties of polycrystalline samples of the intrinsic magnetic topological insulators $MnPn_2Te_4$, with pnictogen Pn = Sb, Bi, by bulk magnetization and μSR. DC susceptibility detects the onset of magnetic ordering at T_N = 27 K and 24 K and a field dependence of the macroscopic magnetization compatible with ferri- (or ferro-) and atiferro- magnetic ordering, respectively. Weak transverse field (wTF) Muon Spin Rotation (μSR) confirms the homogeneous bulk nature of magnetic ordering at the same two distinct transition temperatures. Zero Field (ZF) μSR shows that the Sb based material displays a broader distribution of internal field at the muon, in accordance with a larger deviation from the stoichiomectric composition and a higher degree of positional disorder (Mn at the Pn(6c) site), which however does not affect significantly the sharpness of the thermodynamic transition, as detected by the muon magnetic volume fraction and the observability of a critical divergence in the longitudinal and transverse muon relaxation rates.

1. Introduction

Topological quantum materials have drawn significant attention by both solid state chemistry and physics as they promise potentially useful applications like more energy-efficient microelectronic components, better catalysts, and improved thermometric converters[1, 2]. Importantly, the addition of magnetic ions in materials already displaying non-trivial topology in their electronic structure can leverage on the spin-orbit coupling to realize novel quantum spin phenomena such as the quantum anomalous Hall effect (QAHE)[3, 4], the hallmark of a new generation of materials for powerful spin-based electronics.

The first attempts in this direction where obtained by diluting magnetic ions in few topological insulator material platforms, for instance observing the QAHE in Cr- or V-doped $(Bi,Sb)_2Te_3$, [5, 6, 7]. Only recently nearly stoichiometric magnetic topological insulators (MTIs) such as $MnBi_2Te_4$, displaying QAHE, were synthesized and have thus been proposed as a more robust platform [8]. These systems are van der Waals compounds, exploiting the weak nature

of certain inter-layer London forces in order to produce a family of natural hetrostructures $(MnPn_2Te_4)(Pn_2Te_3)_n$, realized experimentally for instance in the case of Pn = Bi with $n = 0, 1, 2, 3, 4$ and thus proposed as an example of intrinsic MTI. [9, 10, 11, 12]

In this material both magnetic order and a topologically nontrivial band structure coexist. $MnBi_2Te_4$ (n=0) is composed of septuple layer blocks of Te-Bi- Te-Mn-Te-Bi-Te stacked along the [0001] direction and weakly bound to each other by van der Waals forces. It develops an interlayer antiferromagnetic state below 25K, in which ferromagnetic Mn layers of neighbouring blocks are coupled antiferromagnetically, with the easy axis of the staggered magnetization perpendicular to the layers (along the c-axis)[10].

This composition displays a purely antiferromagnetic behaviour below T_N (no field dependent increase of the magnetization), although a lower metamagnetic transition does develop a finite bulk magnetic moment. ARPES measurements on $MnBi_2Te_4$ show clear evidence of surface states with a gap of 30 meV at the Dirac point. Most surprisingly, this gap survives well above the magnetic transition temperature [13] The origin of this feature remains unclear, but was recently attributed to short-range magnetic field generated by chiral spin fluctuations[14]. Another possibility behind the fact that the gap persists up to high temperature could be that the magnetic order at the surface is different than the bulk, e.g. has a significantly higher transition temperature.

A sister compound $MnSb_2Te_4$ has been synthesized along similar lines, displaying a magnetic ground state and magnetic ordering temperature[15, 16], albeit with distinct differences with respect to $MnBi_2Te_4$. Due to the similar ionic radii and almost identical coordination environment of Mn^{2+} and Sb^{3+} ions, $MnSb_2Te_4$ exhibits very notable cationic intermixing: Mn and Sb atoms, nominally in crystallographic Wyckoff positions 3a and 6c, respectively, can both swap their positions [16, 17]. As a consequence the magnetic transition temperature varies from 19 K to well above 40 K, while the magnetic ground state changes from antiferromagnetic to a ferro/ferrimagnetic, influenced by stoichiometry, and depending on synthesis conditions. [18] All samples display a smaller moment at saturation than expected from the formal Mn^{2+} valence (≈ 2 instead of 5.9 μ_B). The actual composition determined by a combination of X-ray diffraction methods and energy-dispersive X-ray spectroscopy turns out to be $Mn_{1-y}Sb_{2-y}Mn_yTe_4$, generally with a finite departure from ideal stoichiometry and a correlation between total Mn site occupancy, $1 - y$, and the ordering temperature.

Several macroscopic bulk and surface magnetometry study have been reported but no results from microscopic local probes of magnetism have been published to date. Hence it is crucial to get insight on magnetic ordering though sensitive local spectroscopic technique like μSR. Here we studied the magnetic ordering of the same polycrystalline samples of $MnBi_2Te_4$ and $MnSb_2Te_4$ by Superconducting Quantum Interference Device (SQUID) magnetometry and μSR.

2. Experimental methods

Pressed pellets of nominal $MnBi_2Te_4$ and $MnSb_2Te_4$ were prepared by the solid state synthesis method in TU Dresden,Germany.

The DC magnetic susceptibility measurements were conducted with commercial Quantum Design SQUID magnetometers equipped with a vibrating sample magnetometer option (SQUID-VSM and MPMS3).

All the μSR experiments were carried out on the GPS spectrometer, at Paul Scherrer Institute, Villigen, Switzerland. Polycrystalline pressed pellets of both the samples were measured in WTF and ZF. All the measurements were carried out using a ^{4}He-flow cryostat with samples mounted on standard sample holders.

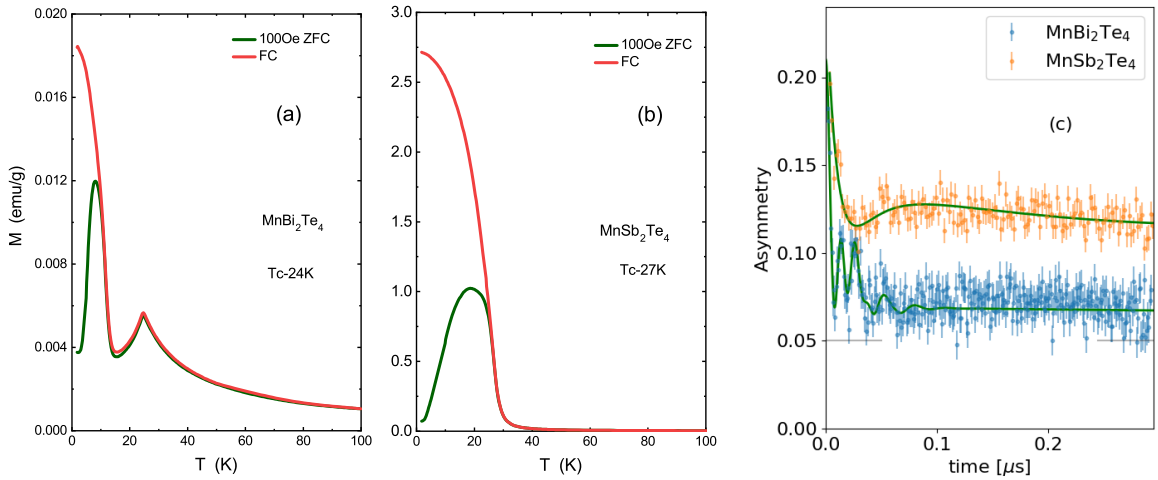

Figure 1. Temperature dependence of magnetic moment in (a) $MnBi_2Te_4$and (b) $MnSb_2Te_4$; (c) ZF μSR spectra of both at 5K.

3. Results and Discussion

Bulk DC magnetization measurements on $MnBi_2Te_4$ and $MnSb_2Te_4$ are shown in Fig. 1. Panel (a) shows the temperature dependence of the $MnBi_2Te_4$ magnetic moment $m(T)$ measured in a small applied magnetic field (100 Oe), both cooling in the field (FC) and on warming the sample, applying the field after cooling in zero Oe (ZFC). Upon decreasing the temperature the FC curve shows a sharp cusp at 24 K, insensitive to the FC/ZFC protocol, followed by a second upturn at low temperature, whose magnitude is protocol dependent. This indicates an antiferromagnetic ordering below $T_N = 24$ K and a metamagnetic transition at $T^* = 11$ K to ferromagnetic-like order at low temperatures. It is clear from previous reports [10] that antiferromagnetism is due to the sign of the inter-layer exchange interaction between the Mn^2+ ion at the 3a Wyckoff position. However, the origin of ferromagnetic like interaction is still elusive which is observed for the first time in our sample.

The magnetization of the second sample, $MnSb_2Te_4$, is shown in Fig. 1(b). Unlike the Pn = Bi sample, by lowering the temperature the splitting of the ZFC and the FC curves occurs together with a sharp increase in the magnetic moment. This indicates a long range ferromagnetic-like order, below T_N= 27K. The origin of a ferromagnetic-like structure is attributed to intermixing. The presence of magnetic ions at the 6c site, mediating either a ferro- or an antiferromagnetic interaction, gives rise in both cases to an effective ferromagnetic inter-layer coupling.[1]

Then starting by considering the results of Zero Field (ZF) μSR measurements, recalling that muon stopping in a polycrystalline sample in the ordered phase give rise to distinct transverse (t) precessing and longitudinal (l) non-precessing components around the internal fields. Figure 1 (c) shows the time dependent ZF asymmetry in $MnBi_2Te_4$ and $MnSb_2Te_4$ at 5K, well below T_N. Here the time dependent asymmetry in $MnBi_2Te_4$ shows clear oscillations representing coherent muon-spin precession around the local field at the implantation site, demonstrating that the sample is in a magnetically ordered state characterized by long-range order at 5K. However, the relaxation rates of these precessions is large. A possible choice of minimal ingredients for the

[1] We still refer to the transition temperature of $MnSb_2Te_4$ as T_N in the assumption that the structure is ferrimagnetic.

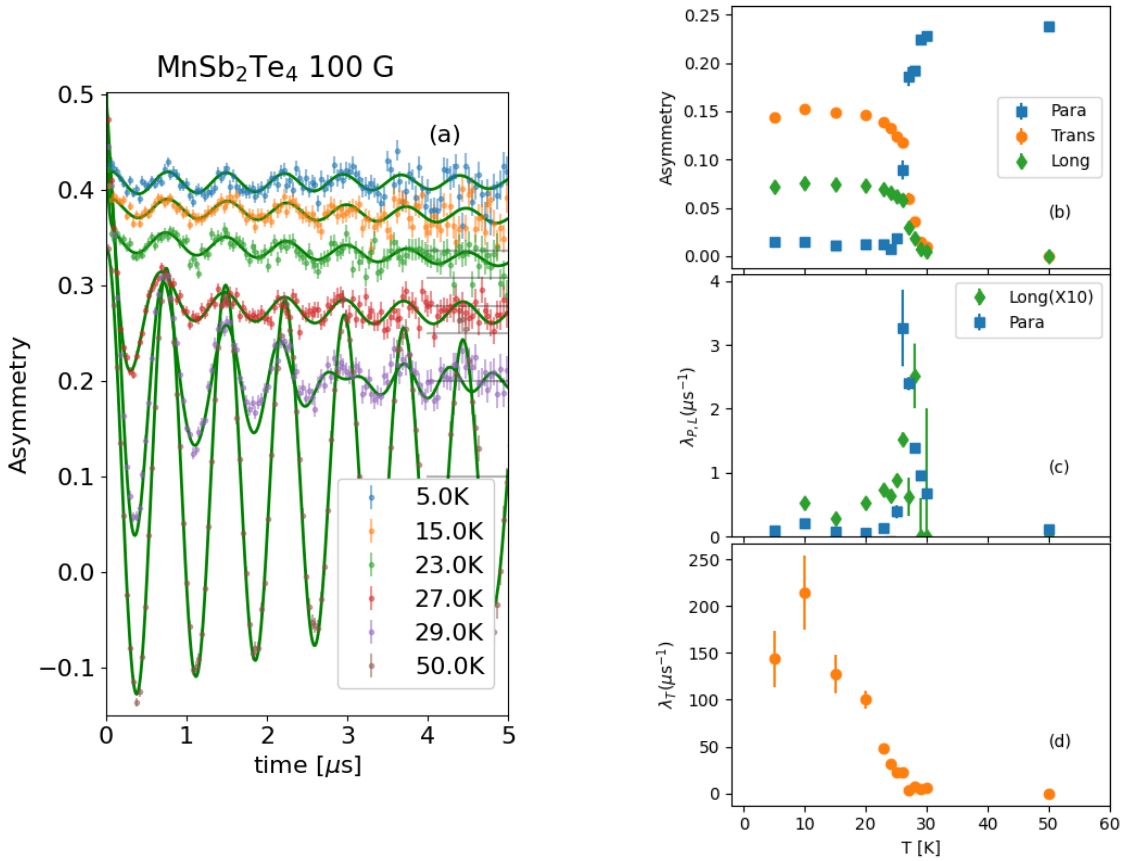

Figure 2. (a)wTF μSR asymmetry vs. time for $MnSb_2Te_4$ for 5 K $\leq T \leq$ 50 K, above and below T_N, shifted vertically for clarity, with best fits; Temperature dependence of wTF best fit parameters, asymmetry (b) slow (c) and fast (d) relaxation rates.

best fit function is the following

$$A_{ZF}(t) = A_0 \left[f_{t1}\, \mathrm{J}_0(\gamma_\mu B_1 t) e^{-\sigma_!^2 t^2/2} + f_{t2}\, \cos(\gamma_\mu B_2 t) e^{-t^2/2T_2^2} + f_{t3}\, e^{-\sigma_3^2 t^2/2} + f_l \exp^{-t/T_1} \right] \quad (1)$$

with three transverse components, representing a broad distribution of fields, with a fast decay (f_{t3}) and two discernible oscillations, here chosen as $f_{t1} J_0$, a Bessel function of the first kind, [19] and f_{t2}, a simple cosine. A_0 is the maximum experimental asymmetry. The fourth term is a longitudinal decay representing the l component, but including a tiny fraction of muons stopping outside the sample, as well. Marginally worse χ^2 values are obtained with two cosine functions and a fast decay for the transverse component.

The time-dependent asymmetry of $MnSb_2Te_4$ displays only overdamped oscillations, indicative of a severe broadening of the field distribution, and fewer ingredients are required in the best fit function

$$A_{ZF}(t) = A_0 \left[f_1\, KT_d(\Delta_1, \nu_1, t) + f_{t2}\, e^{-t^2/2T_2^2} + f_l\, e^{-t/T_1} \right] \quad (2)$$

Here the fraction $f_1\, KT_d$ is a dynamical Kubo-Toyabe function [19], with a small dynamical frequency $\nu_1 = 0.17\,\mu\mathrm{s}^{-1}$, already accounting for its own longitudinal component. The term f_l accounts for both the longitudinal fractions of the fast decay component f_{t2} and for muons

stopping outside the sample. The best fits to Eq. 1 and 2 correspond to the green curves in Fig. 1 (c).

We now report weak Transverse Field (wTF) μSR measurements that feature a full-asymmetry precession in the absence of static internal fields, in the paramagnetic phase. The weak field is however much smaller than internal fields in the ordered phase, where it does not alter the distinction between t and l components, leading to just a tiny wTF precession from the marginal fraction of muons stopping outside the sample.

Figure 2 (a) shows a representative subset of μSR asymmetries vs. time, both above and below $T_N = 27K$, together with best fit curves to the function

$$A_{wTF}(t) = A_p \cos(\gamma B + \phi)\, e^{-\lambda_p t} + A_t\, e^{-\lambda_t t} + A_l\, e^{-\lambda_l t} \tag{3}$$

Well below T_N only the few muons stopping in the sample environment contribute to the precessing p term with a constant value $A_e = 0.015$, and the two further terms represent the fast decaying t and the slow decaying l sample components. Above T_N the whole sample is contributing to the p (for paramagnetic) term, whose value is the maximum experimental asymmetry A_0. The temperature dependence of the best fit parameters is shown in Fig. 2: panel (b) shows asymmetries, confirming that $A_l + A_t + Ap = A_0$ at all temperatures, while $A_l \approx A_t/2$ for $T \to 0$, as expected from polycrystalline ordered magnets, with an abrupt transition $A_t(T) + A_l(T) \to 0$ for $T > T_N$. The transition is also marked by a relatively sharp divergence of the slow relaxation rates λ_p and λ_l, panel (c). Below the transition the rate λ_t, panel (d), representing both the mean internal field and the width of its distribution, grows with decreasing T like an order parameter.

The wider distribution of internal fields in $MnSb_2Te_4$, shown both in ZF (Fig. 1 c) and in wTF (Fig. 2 d) is due to many different local configurations introduced by the larger cationic intermixing, which, however, differently from typical *bad metal* oxides, like cuprates, does not compromise severely the uniqueness of the thermodynamic magnetic transition. This is very clearly pointed out by the magnetic volume fraction, calculated from wTF best fits according to $v_m(T) = 1 - (A_p(T) - A_e)/(A_0 - Ae)$ and shown in Fig. 3.

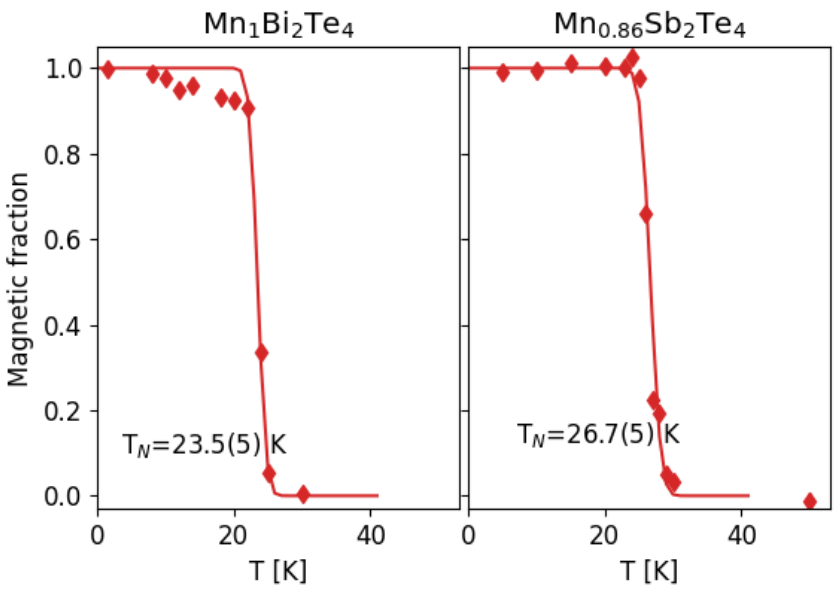

Figure 3. Temperature dependence of magnetic fraction in $MnBi_2Te_4$and $MnSb_2Te_4$

The uniform sampling of powder grains by the implanted muons thus provides an important information on the nature of the phase transition. Despite the local disorder witnessed by the internal field distribution, broadest in $MnSb_2Te_4$, both samples behave as a very homogeneous magnet with a sharp transition at $T_N = 23.5(5), 26.7(5)$ K, for Pn = Bi, Sb respectively. The residual width is compatible with an average composition variance among powder grains.

This non trivial conclusion is confirmed for Pn = Sb also by the other wTF best fit parameters, displayed in the two lower panels of Fig. 2. The internal field represented by the faster relaxation rate drops to zero at the same value of T_N. More significantly, critical divergence of the longitudinal relaxation rate is easily washed out in the presence of disorder, whereas its observation in the Sb based sample confirms a well defined, unique transition. Zero Field μSR best fits at different temperatures (not reported) confirm this statement.

4. Conclusions

We investigated two sister materials in the very promising MTI candidate system $MnPn_2Te_4$. SQUID and μSR measurements agree on the ordering transition temperature in both $MnBi_2Te_4$ and $MnSb_2Te_4$. The two compounds display distinct magnetic behaviours, attributed to antiferro- and ferrimagnetic ordering, respectively. The difference is correlated to the influence of cation intermixing between the Mn and the Pn ion, which is more relevant for the Sb compound and correlates with a broader width of the distribution of internal fields determined by μSR. The large width witnesses an intrinsic source of disorder which is much more pronounced in the Sb sample. The contrast between large field widths and sharp transition in the magnetic volume fraction from muon spectroscopy demonstrates that disorder is not deterimental for very homogeneous magnetic properties in the MTI candidate materials.

Acknowledgments

We acknowledge the help of Dr.Chennan Wang during the μSR experiments, also during pandemic period. This work was supported by the Deutsche Forschungsgemeinschaft (DFG) within the Würzburg-Dresden Cluster of Excellence on Complexity and Topology in Quantum Matter – *ct.qmat* (EXC 2147, project-id 390858490).

References

[1] Luo H, Yu P, Li G and Yan K 2022 *Nature Reviews Physics* 1–14
[2] Kumar N, Guin S N, Manna K, Shekhar C and Felser C 2020 *Chemical Reviews* **121** 2780–2815
[3] Tokura Y, Yasuda K and Tsukazaki A 2019 *Nature Reviews Physics* **1** 126–143
[4] Wang P, Ge J, Li J, Liu Y, Xu Y and Wang J 2021 *The Innovation* **2** 100098
[5] Chang C Z, Zhang J, Feng X, Shen J, Zhang Z, Guo M, Li K, Ou Y, Wei P, Wang L L *et al.* 2013 *Science* **340** 167–170
[6] Chang C Z, Zhao W, Kim D Y, Zhang H, Assaf B A, Heiman D, Zhang S C, Liu C, Chan M H and Moodera J S 2015 *Nature materials* **14** 473–477
[7] Bestwick A, Fox E, Kou X, Pan L, Wang K L and Goldhaber-Gordon D 2015 *Physical Review Letters* **114** 187201
[8] Liu C, Wang Y, Li H, Wu Y, Li Y, Li J, He K, Xu Y, Zhang J and Wang Y 2020 *Nature Materials* **19** 522–527
[9] Klimovskikh I I, Otrokov M M, Estyunin D, Eremeev S V, Filnov S O, Koroleva A, Shevchenko E, Voroshnin V, Rybkin A G, Rusinov I P *et al.* 2020 *npj Quantum Materials* **5** 1–9
[10] Otrokov M M, Klimovskikh I I, Bentmann H, Estyunin D, Zeugner A, Aliev Z S, Gaß S, Wolter A, Koroleva A, Shikin A M *et al.* 2019 *Nature* **576** 416–422
[11] Hao Y J, Liu P, Feng Y, Ma X M, Schwier E F, Arita M, Kumar S, Hu C, Zeng M, Wang Y *et al.* 2019 *Physical Review X* **9** 041038
[12] Shi M, Lei B, Zhu C, Ma D, Cui J, Sun Z, Ying J and Chen X 2019 *Physical Review B* **100** 155144
[13] Vidal R, Bentmann H, Peixoto T, Zeugner A, Moser S, Min C H, Schatz S, Kißner K, Ünzelmann M, Fornari C *et al.* 2019 *Physical Review B* **100** 121104

[14] Shikin A M, Estyunin D, Klimovskikh I I, Filnov S, Schwier E, Kumar S, Miyamoto K, Okuda T, Kimura A, Kuroda K *et al.* 2020 *Scientific Reports* **10** 1–13
[15] Wimmer S, Sánchez-Barriga J, Küppers P, Ney A, Schierle E, Freyse F, Caha O, Michalička J, Liebmann M, Primetzhofer D *et al.* 2021 *Advanced Materials* **33** 2102935
[16] Folkers L C, Corredor L T, Lukas F, Sahoo M, Wolter A U and Isaeva A 2021 *Zeitschrift für Kristallographie-Crystalline Materials*
[17] Liu Y, Wang L L, Zheng Q, Huang Z, Wang X, Chi M, Wu Y, Chakoumakos B C, McGuire M A, Sales B C *et al.* 2021 *Physical Review X* **11** 021033
[18] Yan D, Yang M, Song P, Song Y, Wang C, Yi C and Shi Y 2021 *Physical Review B* **103** 224412
[19] Blundell S J, De Renzi R, Lancaster T and Pratt F L 2021 *Muon Spectroscopy: An Introduction* (Oxford University Press) ISBN 9780198858959 (*Preprint* `https://academic.oup.com/book/43671/book-pdf/44866003/oso-9780198858959.pdf`) URL `https://doi.org/10.1093/oso/9780198858959.001.0001`